Piecewise linear emulation of propagating fronts as a method for determining their speeds

Stavros Theodorakis* and Efthymios Svoukis
Physics Department, University of Cyprus, P.O. Box 20537, Nicosia 1678, Cyprus

(Received 26 March 2003; published 15 August 2003)

We use piecewise linear terms to emulate the polynomial nonlinear terms in a typical reaction-diffusion equation, replacing it thus with a set of simple linear inhomogeneous differential equations. The resulting analytic solution constitutes an excellent approximation to the exact propagating front, as is explicitly shown in the case of cubic and quintic nonlinearities, yielding also the correct value for the physically selected speed of the observable front. Such a piecewise linear emulation can be used for any nonlinearity, giving therefore a very reliable and accurate method for determining the selected speed of fronts invading unstable states, especially pushed fronts.

DOI: 10.1103/PhysRevE.68.027201 PACS number(s): 05.45.−a, 64.60.Qb, 64.60.Ht, 82.40.Fp

In many systems rendered suddenly unstable, propagating fronts appear. The determination of the speed of a front propagating into an unstable state has attracted a lot of attention. The selection principles that have been formulated to determine the observable front, without having to solve directly the partial differential equation of motion for a range of initial conditions, have involved concepts of linear and nonlinear marginal stability, of structural stability and of causality [1,2]. Even though a complete analytical understanding of the propagation mechanism and relaxation behavior has emerged for those fronts that are "pulled along" by the spreading of linear perturbations about the unstable state, the so-called "pulled" fronts [3], the case of those fronts where linear analysis fails, the so-called "pushed" fronts, is still the subject of ongoing research. There is no universal way for dealing with pushed fronts, whether analytical or numerical; there are, however, some methods applicable to a few special cases [1].

In previous papers [4], we have presented a speed selection mechanism that applies to fronts invading both unstable and metastable states, whether they be pulled or pushed, and that works even for fields propagating at different speeds. Still, the mechanism had to rely mostly on numerical calculations, since the nonlinearities encountered are almost never analytically tractable. These numerical calculations become quite cumbersome when there are parameters involved.

In this paper, we find the selected speed of pushed fronts through analytic calculations, having approximated all nonlinearities by piecewise linear terms. The approximation of nonlinearities by linear pieces has been used before in other contexts [5]. More generally, the idea of solving nonlinear boundary value problems by approximating terms of the differential equation and then patching local solutions at the knots has been used for finding numerical solutions to a number of boundary value problems [6]. We use this idea here in order to obtain the selected speed from analytic approximate solutions for the propagating fronts.

Let us consider, for example, Fisher's dimensionless reaction-diffusion equation

$$\frac{\partial \phi}{\partial t} = \frac{\partial^2 \phi}{\partial x^2} + f(\phi), \tag{1}$$

where $f(p)=f(0)=0$, the fixed point 0 being an unstable state. If the field is going to have a monotonic front $\phi(\xi)$, where $\xi = x - vt$, then

$$\frac{d^2 \phi}{d\xi^2} + v\frac{d\phi}{d\xi} + f(\phi) = 0. \tag{2}$$

We shall be solving this "steady state" equation, numerically or otherwise, in a large *finite* interval $[L_1, L_2]$, with $L_1 \ll L_2$, subject to the boundary conditions $\phi(L_1)=p$ and $\phi(L_2)=0$. For any given value of v, we can find a unique solution. The selected speed is found by letting $-L_1$ and L_2 go to infinity at the end of the calculation [4].

Let us now consider that part of $f(\phi)$ in Eq. (2) that is strictly nonlinear. We can plot this nonlinearity as a function of ϕ and can then approximate the resulting curve by a set of linear segments tangent to the original curve. We replace, in other words, the nonlinear function by a piecewise linear one, consisting of pieces tangent to the original curve. If these pieces are infinite in number, clearly the two curves will coincide. In practice though we shall keep only a few linear segments, the positions of which are chosen so as to ensure that the area between the polygonal curve and the original nonlinear curve is minimized. We say then that we have constructed a piecewise linear emulator of the nonlinearity. As a result, the nonlinear ordinary differential equation can be replaced by a set of linear inhomogeneous differential equations, which can be solved analytically. The various constants involved will be determined by requiring that ϕ be continuous and smooth everywhere. The resulting algebraic equations can be handled through symbolic calculations and will easily yield the value of the speed. All we need to do is write down the equations that take into account the boundary conditions and the continuity conditions, let the ends of the interval go to infinity and then solve the corresponding algebraic equations, symbolically or numerically. In practice, the speed obtained and the corresponding solution are very accurate even when only a few segments make up the polygonal emulator curve.

*Electronic address: stavrost@ucy.ac.cy

 ©2003 The American Physical Society

We shall demonstrate this piecewise linear emulation by examining two particular reaction-diffusion equations, for which the selected speed is known. We shall see that the emulation yields highly accurate results, obtained in a rather straightforward manner by using the resulting analytic expressions.

Let us examine a specific case of the Fisher equation

$$\frac{d^2\phi}{d\xi^2}+v\frac{d\phi}{d\xi}+\phi-g(\phi)=0, \tag{3}$$

where the nonlinear polynomial $g(\phi)$ will be assumed to be cubic or quintic. In this paper, we shall illustrate the main ideas of our work by focusing on the cases $g(\phi)=g_c(\phi)=[\phi^3-(1-b)\phi^2]/b$ and $g(\phi)=g_q(\phi)=\phi^5-d\phi^3$. Here b and d are given parameters.

In the cubic case, $g(\phi)=g_c(\phi)$, the selected speed is known [7] to be $v_c^*=\sqrt{2b}+(1/\sqrt{2b})$ when $0\leqslant b\leqslant 1/2$ (pushed case), while the exact corresponding front is

$$\phi(\xi)=\frac{1}{2}-\frac{1}{2}\tanh(\xi/\sqrt{8b}). \tag{4}$$

For the quintic case, where $g(\phi)=g_q(\phi)$, the selected speed is known [1] to be $v_q^*=(-d+2\sqrt{d^2+4})/\sqrt{3}$ when $d\geqslant 2/\sqrt{3}$ (pushed case), while the exact corresponding front is

$$\phi(\xi)=(e^{2\xi p_q^2/\sqrt{3}}+p_q^{-2})^{-1/2}, \tag{5}$$

with $p_q=(d+\sqrt{d^2+4})^{1/2}/\sqrt{2}$.

The basic idea of the present paper is to replace the nonlinear function $g(\phi)$ with an emulator function $w(\phi)$ and then solve Eq. (3). We shall see that in both the cubic and the quintic cases, the results of the emulation constitute an excellent approximation to the exact results.

Let us begin by obtaining the emulator functions in the two cases. In both cases, function $g(\phi)$ begins at $\phi=0$. As ϕ increases $g(\phi)$ becomes negative, passes through an inflection point and then reaches a minimum value at ϕ_0. Afterwards, it increases monotonically. The field ϕ satisfies the boundary conditions $\phi(L_1)=p$ and $\phi(L_2)=0$, where the fixed point p is equal to 1 in the cubic case and to $p_q=(d+\sqrt{d^2+4})^{1/2}/\sqrt{2}$ in the quintic case.

The shape of $g(\phi)$ is such that a polygonal curve will have to consist of quite a few linear segments if it is going to look like the $g(\phi)$ curve. Indeed, it seems that three segments will be needed on the left of the minimum ϕ_0. These segments will be tangent to $g(\phi)$ at the points 0, s, and ϕ_0. On the right of the minimum, three segments will be needed as well. These segments will be tangent to $g(\phi)$ at the points p, t, and ϕ_0. Thus, there are five segments in all. The points s and t will be chosen so as to minimize the area between the emulator curve and the original curve.

Then the emulator curve that consists of five linear segments, all of them tangent to $g(\phi)$, will be

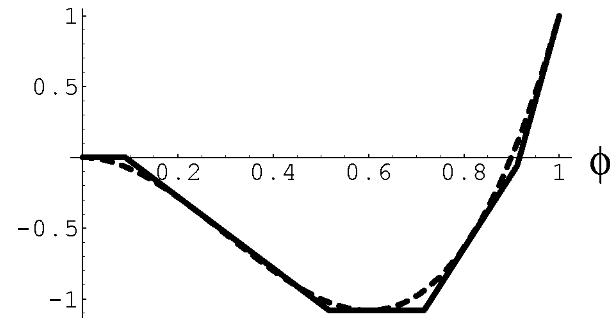

FIG. 1. The cubic function $g_c(\phi)$, represented by the dashed line, and its piecewise linear emulator $w_c(\phi)$, represented by the continuous line, for $b=0.1$. The line segments are tangent to the curve at the points $\phi=0$, $\phi=s=0.248\,882(1-b)$, $\phi=\phi_0=2(1-b)/3$, $\phi=t$, and $\phi=1$, where t is given by Eq. (8).

$$w(\phi)\begin{cases} 0 & \text{if} \quad 0\leqslant\phi\leqslant\phi_1, \\ g'(s)\phi+g(s)-g'(s)s & \text{if} \quad \phi_1\leqslant\phi\leqslant\phi_2, \\ g(\phi_0) & \text{if} \quad \phi_2\leqslant\phi\leqslant\phi_3, \\ g'(t)\phi+g(t)-g'(t)t & \text{if} \quad \phi_3\leqslant\phi\leqslant\phi_4, \\ g'(p)\phi+g(p)-g'(p)p & \text{if} \quad \phi_4\leqslant\phi\leqslant p, \end{cases} \tag{6}$$

where

$$\phi_1=s-[g(s)/g'(s)],$$

$$\phi_2=s+[g(\phi_0)-g(s)]/g'(s),$$

$$\phi_3=t+[g(\phi_0)-g(t)]/g'(t),$$

$$\phi_4=\frac{g(t)-g'(t)t-g(p)+g'(p)p}{g'(p)-g'(t)}. \tag{7}$$

The values of the functions $g(\phi)$ and $w(\phi)$ are the same at points 0, s, ϕ_0, t, and p, and so are their slopes at these points. The point s, located in the interval $[\phi_1,\phi_2]$, and the point t, located in the interval $[\phi_3,\phi_4]$, will be chosen so as to make the emulator as similar as possible to the original.

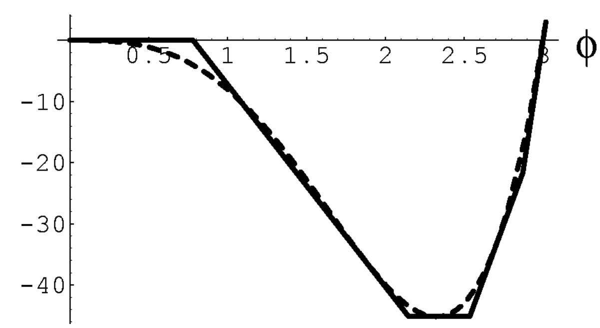

FIG. 2. The quintic function $g_q(\phi)$ and its piecewise linear emulator $w_q(\phi)$, for $d=9$. The line segments are tangent to the curve at the points $\phi=0$, $\phi=s=1.8774$, $\phi=\phi_0=2.3238$, $\phi=t=2.703\,77$, and $\phi=p_q=3.018$. The dashed curve corresponds to the function $g_q(\phi)$, while the continuous curve corresponds to its piecewise linear emulator.

They are thus determined by requiring that the area between the emulator curve and the $g(\phi)$ curve be minimized.

In the cubic case, where $g(\phi)=g_c(\phi)=[\phi^3-(1-b)\phi^2]/b$, it turns out that $s=0.248\,882(1-b)$ and $\phi_0=2(1-b)/3$, while

$$t=-\frac{b}{3}+\frac{\sqrt{2+b+b^2}}{3}[\cos(\theta/3)+\sqrt{3}\sin(\theta/3)], \quad (8)$$

where $\theta=\cos^{-1}[(3b^2+3b-0.5)/(2+b+b^2)^{3/2}]$. The resulting emulator curve is a very good simulacrum of the original curve $g_c(\phi)$, as seen in Fig. 1.

In the quintic case, where $g(\phi)=g_q(\phi)=\phi^5-d\phi^3$, it turns out that $s=0.625\,792\sqrt{d}$ and $\phi_0=\sqrt{3d/5}$, the expression for the parameter t being more cumbersome. The resulting emulator curve is again a very good simulacrum of the original curve $g_q(\phi)$, as seen in Fig. 2.

Having obtained the emulator functions $w_c(\phi)$ and $w_q(\phi)$ for the cubic and quintic cases, respectively, we may now proceed to the solution of the emulated reaction-diffusion problem,

$$\frac{d^2\phi}{d\xi^2}+v\frac{d\phi}{d\xi}+\phi-w(\phi)=0, \quad (9)$$

subject to the boundary conditions $\phi(L_1)=p$ and $\phi(L_2)=0$. This problem is easy to solve analytically, since it involves linear inhomogeneous differential equations.

Let us define first the parameters

$$u_i=\frac{-v+\sqrt{v^2-4+4g'(\chi_i)}}{2} \quad (10)$$

and

$$z_i=\frac{-v-\sqrt{v^2-4+4g'(\chi_i)}}{2}, \quad (11)$$

where $\chi_4=p$, $\chi_3=t$, $\chi_2=\phi_0$, and $\chi_1=s$. Then the solution of Eq. (9) is

$$\phi(\xi)=p+(\phi_4-p)\frac{e^{u_4(\xi-L_1)}-e^{z_4(\xi-L_1)}}{e^{u_4(\xi_4-L_1)}-e^{z_4(\xi_4-L_1)}} \quad \text{if} \quad L_1\leqslant\xi\leqslant\xi_4,$$

$$\phi(\xi)=\Lambda+(\phi_3-\Lambda)\frac{e^{u_3(\xi-\xi_4)}-e^{z_3(\xi-\xi_4)}}{e^{u_3(\xi_3-\xi_4)}-e^{z_3(\xi_3-\xi_4)}}+(\phi_4-\Lambda)\times\frac{e^{u_3(\xi_3-\xi_4)+z_3(\xi-\xi_4)}-e^{u_3(\xi-\xi_4)+z_3(\xi_3-\xi_4)}}{e^{u_3(\xi_3-\xi_4)}-e^{z_3(\xi_3-\xi_4)}} \quad \text{if} \quad \xi_4\leqslant\xi\leqslant\xi_3,$$

$$\phi(\xi)=g(\phi_0)+[\phi_2-g(\phi_0)]\frac{e^{u_2(\xi-\xi_3)}-e^{z_2(\xi-\xi_3)}}{e^{u_2(\xi_2-\xi_3)}-e^{z_2(\xi_2-\xi_3)}}+[\phi_3-g(\phi_0)]\times\frac{e^{u_2(\xi_2-\xi_3)+z_2(\xi-\xi_3)}-e^{u_2(\xi-\xi_3)+z_2(\xi_2-\xi_3)}}{e^{u_2(\xi_2-\xi_3)}-e^{z_2(\xi_2-\xi_3)}} \quad \text{if} \quad \xi_3\leqslant\xi\leqslant\xi_2,$$

$$\phi(\xi)=M+(\phi_1-M)\frac{e^{u_1(\xi-\xi_2)}-e^{z_1(\xi-\xi_2)}}{e^{u_1(\xi_1-\xi_2)}-e^{z_1(\xi_1-\xi_2)}}+(\phi_2-M)\times\frac{e^{u_1(\xi_1-\xi_2)+z_1(\xi-\xi_2)}-e^{u_1(\xi-\xi_2)+z_1(\xi_1-\xi_2)}}{e^{u_1(\xi_1-\xi_2)}-e^{z_1(\xi_1-\xi_2)}} \quad \text{if} \quad \xi_2\leqslant\xi\leqslant\xi_1,$$

$$\phi(\xi)=\phi_1\frac{e^{u_2(\xi-L_2)}-e^{z_2(\xi-L_2)}}{e^{u_2(\xi_1-L_2)}-e^{z_2(\xi_1-L_2)}} \quad \text{if} \quad \xi_1\leqslant\xi\leqslant L_2, \quad (12)$$

where $\Lambda=[g(t)-g'(t)t]/[1-g'(t)]$ and $M=[g(s)-g'(s)s]/[1-g'(s)]$.

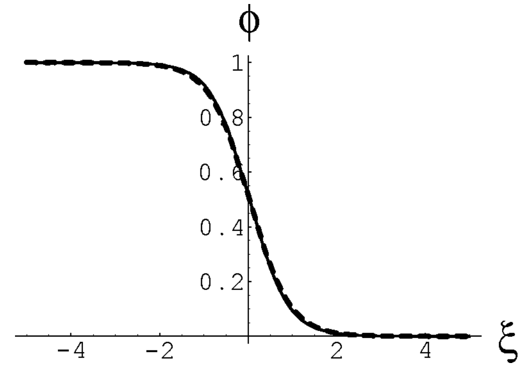

FIG. 3. The selected front in the cubic case, for $b=0.1$. The continuous line shows the result given by the piecewise linear emulation, while the dashed line shows the exact result.

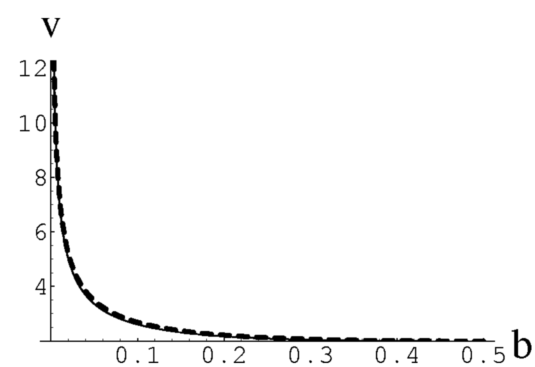

FIG. 4. The selected speed v in the cubic case for $0\leqslant b\leqslant 1/2$ (pushed case). The dashed line shows the exact result, while the continuous line shows the result given by the piecewise linear emulation.

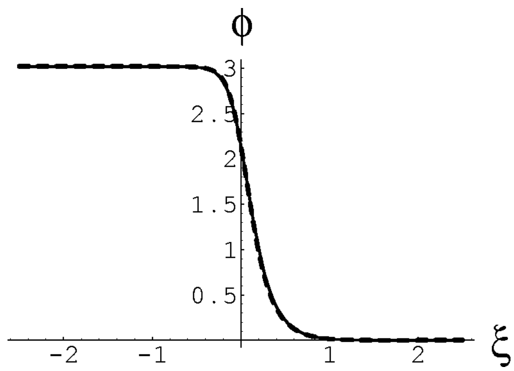

FIG. 5. The selected front in the quintic case, for $d=9$. The continuous line shows the result given by the piecewise linear emulation, while the dashed line shows the exact result.

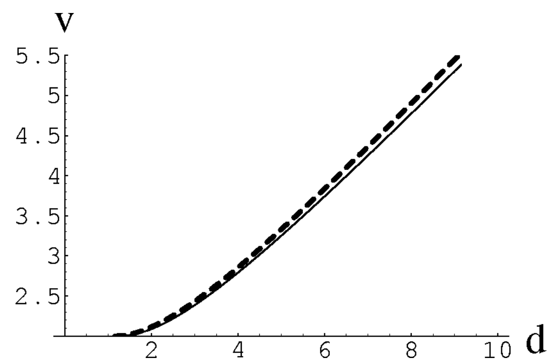

FIG. 6. The selected speed v in the quintic case for $d \geqslant 2/\sqrt{3}$ (pushed case). The dashed line shows the exact result, while the continuous line shows the result given by the piecewise linear emulation.

This function is continuous everywhere and it acquires the values p, ϕ_4, ϕ_3, ϕ_2, ϕ_1, and 0 at points $\xi=L_1$, $\xi=\xi_4$, $\xi=\xi_3$, $\xi=\xi_2$, $\xi=\xi_1$, and $\xi=L_2$, respectively. The continuity of the slope of $\phi(\xi)$ at points $\xi=\xi_1$, $\xi=\xi_2$, $\xi=\xi_3$, and $\xi=\xi_4$ yields the parameters ξ_1, ξ_2, ξ_3, and ξ_4. Thus, the function $\phi(\xi)$ is completely determined, for arbitrary given values of speed v and of L_1, L_2. If, however, we want the resulting solution to represent a front, we must let $-L_1$ and L_2 tend to infinity. We can easily verify that in that case the four equations that result from the continuity of $d\phi/d\xi$ at points $\xi=\xi_1$, $\xi=\xi_2$, $\xi=\xi_3$, and $\xi=\xi_4$ will depend on the parameters ξ_1, ξ_2, ξ_3, and ξ_4 only through differences of the form $\xi_i-\xi_j$. There are three independent such differences. Three of the four equations will determine these differences as functions of v. The fourth one will determine the speed selected by the front.

It is quite straightforward to solve the four slope equations mentioned above for both the cubic and the quintic cases. The results obtained are compared with the exact ones in Figs. 3, 4, 5, and 6. In the cubic case, for example, we find that the emulated front coincides absolutely with the exact front of Eq. (4), as shown in Fig. 3. An advantage of the method presented in this paper is that it can easily take into account the dependence of the selected speed on various parameters, such as b in the cubic case and d in the quintic case. In particular, it is quite straightforward to calculate the selected speed in the cubic case as a function of the parameter b. As shown in Fig. 4, the selected speed given by the piecewise linear emulation coincides precisely with the exact speed $v_c^* = \sqrt{2b} + (1/\sqrt{2b})$ when $0 \leqslant b \leqslant 1/2$ (pushed case). Similarly, in the quintic case, we find that the emulated front coincides absolutely with the exact front of Eq. (5), as shown in Fig. 5. As far as the selected speed in the quintic case is concerned, Fig. 6 shows that the speed given by the piecewise linear emulation coincides almost exactly with the exact speed $v_q^* = (-d + 2\sqrt{d^2+4})/\sqrt{3}$, where $d \geqslant 2/\sqrt{3}$ (pushed case). Thus, the analytic expressions given by the piecewise linear emulation determine the selected speeds correctly and constitute an excellent approximation to results obtained normally only through extensive numerical work.

[1] W. van Saarloos, Phys. Rev. A **39**, 6367 (1989).
[2] G.C. Paquette, L.Y. Chen, N. Goldenfeld, and Y. Oono, Phys. Rev. Lett. **72**, 76 (1994); G.C. Paquette and Y. Oono, Phys. Rev. E **49**, 2368 (1994); J.M. Chomaz and A. Couairon, Phys. Rev. Lett. **84**, 1910 (2000).
[3] U. Ebert and W. van Saarloos, Physica D **146**, 1 (2000).
[4] S. Theodorakis and E. Leontidis, Phys. Rev. E **62**, 7802 (2000); **65**, 026122 (2002).
[5] H.P. McKean, Adv. Math. **4**, 209 (1970); J. Rinzel and J.B. Keller, Biophys. J. **13**, 1313 (1973); T. Ohta, M. Mimura, and R. Kobayashi, Physica D **34**, 115 (1989); S. Koga, *ibid.* **84**, 148 (1995); A. Ito and T. Ohta, Phys. Rev. A **45**, 8374 (1992); P. Schutz, M. Bode, and V.V. Gafiichuk, Phys. Rev. E **52**, 4465 (1995); E.P. Zemskov, V.S. Zykov, K. Kassner, and S.C. Muller, Nonlinearity **13**, 2063 (2000).
[6] R.C.Y. Chin and R. Krasny, SIAM (Soc. Ind. Appl. Math.) J. Sci. Stat. Comput. **4**, 229 (1983).
[7] E. Ben-Jacob, H. Brand, G. Dee, L. Kramer, and J.S. Langer, Physica D **14**, 348 (1985).